



# Titanium Dioxide and Polyethylmethacrylate electrospun nanofibers: assessing the technique parameters and morphological characterization

Nanofibras eletrofiadas de dióxido de titânio e polietilmetacrilato : avaliação dos parâmetros da técnica e caracterização morfológica

Jessica Dias SANTOS<sup>1</sup>, Tabata Prado SATO<sup>1</sup>, Aline Lins de LIMA<sup>1</sup>, Andrea Souza NOGUEIRA<sup>2</sup>, Cristiane Campos Costa QUISHIDA<sup>2</sup>, Alexandre Luiz Souto BORGES<sup>1</sup>

1 – São Paulo State University (Unesp) – Institute of Science and Technology, São José dos Campos – Department of Dental Materials and Prosthodontics – SP – Brazil.

2 – São Paulo State University (Unesp) – Institute of Science and Technology, São José dos Campos – SP – Brazil.

## ABSTRACT

This work studied the synthetization and morphological characterization of Polyethylmethacrylate (PEMA) nanofibers (NFs) containing titanium dioxide (TiO<sub>2</sub>) produced by the electrospinning technique. The solution to produce the nanofibers was prepared by dissolving 2.5g PEMA in 6.75mL of 1.1.2.2- tetrachloroethane and 3.375mL of dimethylformamide (DMF), and 0.405g of TiO<sub>2</sub> was added to the solution. The nanofiber production used different distances between the tip of the needle to the collector (10, 12 and 15 cm) and two flow rates (0.05 mLh<sup>-1</sup> and 0.08 mLh<sup>-1</sup>) were employed, while the applied voltage was 17kV. The NF morphology was analyzed by Scanning Electron Microscopy (SEM) and Image J software. We used Fourier Infrared Spectroscopy (FTIR) and Energy Dispersive X-Ray Spectroscopy (EDS) to evaluate the structural properties. All parameters were effective in the NF production, however it was shown that the distance of 12 cm produced the best NFs. The mean diameters showed no statistically significant difference between the samples. The FTIR analysis showed characteristic peaks of PEMA and TiO<sub>2</sub>. It was concluded that the employed method was efficient for NF production containing PEMA and TiO<sub>2</sub>, and the morphological characteristics of the NFs were influenced by the voltage and distance.

## KEYWORDS

Polymer; Fibers; Electrochemistry.

## RESUMO

O presente trabalho estudou a sintetização e a caracterização morfológica de nanofibras (NFs) de polietilmetacrilato (PEMA) contendo dióxido de titânio (TiO<sub>2</sub>) produzidas pela técnica da eletrofiação. A solução para o preparo das nanofibras utilizou 2,5 g de PEMA dissolvidos em 6,75 mL de 1,1,2,2 - tetracloroetano (TCE) e 3,375 mL de dimetilformamida (DMF), em sequência foi adicionado 0,405g de TiO<sub>2</sub> à solução. Para eletrofiação, o equipamento foi constituído por uma fonte de alta tensão, uma seringa plástica com agulha de ponta reta e as NFs obtidas foram coletadas em anteparo metálico a 10, 12 e 15 cm de distância da ponta da agulha. A tensão aplicada foi de 17 kV e o fluxo de ejeção variou de 0.05 mLh<sup>-1</sup> e 0.08 mLh<sup>-1</sup>. O diâmetro e a morfologia das NFs foram avaliados por meio de Microscopia Eletrônica de Varredura (MEV) e pelo software Image J. A Espectroscopia por Transformada de Fourier (FTIR) e a Espectroscopia por energia dispersiva de raios X (EDS) avaliaram as propriedades estruturais. A análise morfológica das micrografias mostrou que a distância de 12cm da ponta da agulha até o coletor produziu as melhores NFs. O FTIR demonstrou picos característicos de PEMA e TiO<sub>2</sub>. Diante dos resultados obtidos podemos concluir que o método empregado foi eficiente para a produção de NFs contendo PEMA e TiO<sub>2</sub> e a variação da tensão e distancia influenciaram na morfologias das NFs.

## PALAVRAS-CHAVE

Polímero; Fibras; Eletroquímica.

## INTRODUCTION

Denture stomatitis (DS) is an inflammation which presents high prevalence in patients total or partial removable prostheses and there has been a high relapse rate after treatment [1]. DS is clinically characterized by the presence of hyperemic central points mainly in the mucosa which maintains intimate contact with an internal surface of the prosthesis, and diffuse erythematous areas and papillary hyperplasia of the palate can also be observed in more advanced cases. DS presents multifactorial etiology and involves systemic and local origin causes. *Candida spp.* infection, especially *Candida albicans*, is considered the main etiological factor [2].

The initial microorganism adhesion to the surfaces of the prostheses is a primordial condition for biofilm formation, an important factor related to the development of pathologies [2]. *Candida* species present high adhesion capacity to mucosal epithelial cells and resins used for dental prostheses [2]. *Candida spp.* adheres to the acrylic resin [1] and turns the inner surface of the prostheses into a microbial reservoir [3]. The dental prosthesis becomes colonized by a complex and consistent biofilm capable of colonizing other regions of the oral cavity [4].

Recent studies have shown great concern in order to avoid the microbial proliferation on the surface of prostheses; thus, agents with antimicrobial capacity have been incorporated into the acrylic resins for preparing the prosthesis base and acrylic resins for relining and fabric conditioners. Among the antimicrobial agents used for this purpose are nanoparticles (NP) of nystatin [5], chlorhexidine NP [6], silver NP [7], copper NP [5] and platinum NP [8].

In addition, titanium dioxide NP (TiO<sub>2</sub>) have been added to biomaterials [9]. Recent studies have shown that TiO<sub>2</sub> exhibits antimicrobial activity against *Candida albicans*, *Staphylococcus aureus*, *Pseudomonas aeruginosa*, *Escherichia coli* and *Lactobacillus acidophilus* [10]. TiO<sub>2</sub> characteristics such as white color, low toxicity, high stability, availability and low cost [11] make TiO<sub>2</sub> an appropriate antimicrobial agent suitable for use in dental materials.

However, although these agents promote a reduction in the microbial adhesion when

incorporated in the resins, a good part of the substances are released over time, causing a decrease or absence in the antimicrobial properties of the material [12]. Given the difficulty of maintaining the antimicrobial agent for prolonged periods in the biomaterials, it is necessary to use other techniques for biomaterial synthesis.

The electrospinning technique has been widely used for producing nanoscale fibers [13] because it is a low-cost, simple and versatile technique for manufacturing NFs [14]. Using this technology, it is possible to produce NFs from polymer solutions which depend on environmental parameters, polymeric solution parameters and processing parameters (voltage, flow rate and distance from the capillary tip to the collector) [15,16].

In this process, a fine jet of polymer is ejected when the electric field applied on the polymeric solution exceeds the surface tension. The jet is elongated, dried by solvent evaporation, and is deposited on a collector as fiber or scaffold [17].

Thus, the aim of this study was to define a synthesis and characterization pattern of poly (ethyl methacrylate) (PEMA) NFs containing TiO<sub>2</sub>.

## MATERIALS AND METHODS

### Preparation and Characterization of PEMA/TiO<sub>2</sub> nanofibers

In this study 2.5 g of the polymer poly (ethyl methacrylate) (PEMA) (Tokuyama Rebase Fast II - Tokuyama Dental Corp., Tokyo, Japan), were dissolved in 6.75 mL of 1,1,2,2-tetrachloroethane (TCE) and 3.375 mL of dimethylformamide (DMF). A solution of PEMA was taken to the magnetic stirrer for 24 hours (Figure 1). 0.405g of the TiO<sub>2</sub> was added in solution of PEMA and the new solution was taken to the magnetic stirrer for 24 hours.

### Synthesis of nanofibers

The electrospinning equipment consisted of a high voltage source, an ejection pump and a plastic needle with a straight-edged needle of 0.7mm of diameter (Figure 1). The produced NFs were collected in aluminum foil. Distances of 10, 12 and 15 cm from the tip of the needle and the collector were analyzed, as well as the flow rates of 0.05 mLh<sup>-1</sup> and 0.08 mLh<sup>-1</sup> maintaining a constant voltage of

17 kV for the synthesis of NFs. The collection time of NFs was 10 minutes for all specimens. Thus, 6 experimental groups were obtained from these conditions (Table 1).

After the NFs were synthesized, the NFs' diameter and morphology were evaluated using Scanning Electron Microscopy (SEM) and Fourier Transform Infrared Spectroscopy (FTIR) to analyze the composition of the elements found on the surface of the specimens.

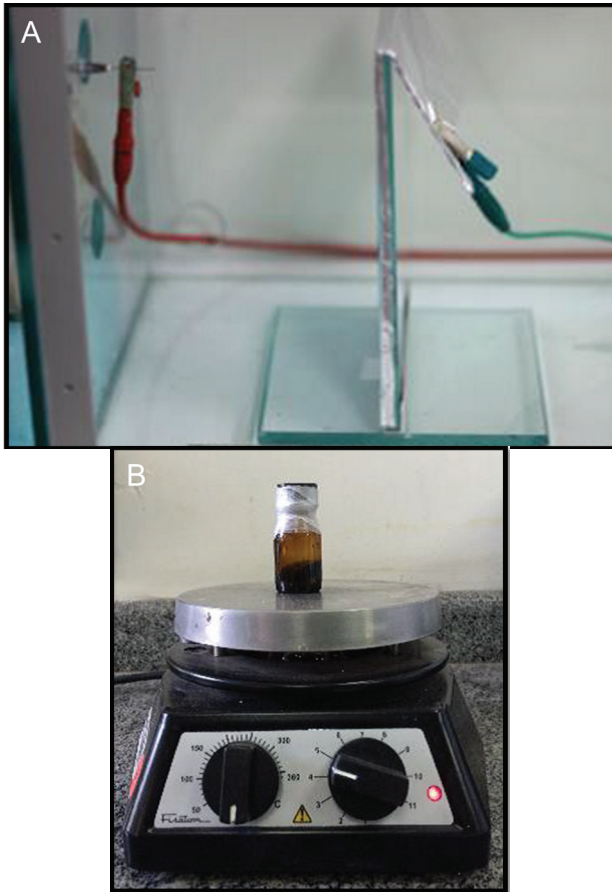


**Figure 1** - PEMA solution was taken to the magnetic stirrer, B. Distance between the ejection pump and a plastic needle.

**Table 1** - Division of each group of nanofibers

Flow Rate (mLh <sup>-1</sup> )	Distance (cm)		
	10	12	15
0.05	G1	G2	G3
0.08	G4	G5	G5

## Characterization of Nanofibers

### Scanning Electron Microscopy (SEM)

After obtaining the specimens, they were fixed in the supports and covered with gold to obtain the microscopic images of the NFs through SEM for morphological evaluation of the obtained NFs.

### Measurement of the nanofiber diameter by Image J software

After obtaining the images by SEM, the diameter of the NFs was measured using ImageJ software. One hundred (100) diameter measurements were performed for each image.

### Fourier Transform Infrared Spectrophotometer (FTIR)

Fourier Transform Infrared Spectrophotometer technique is a standard analytical method often used to characterize the structure of polymers. FT-IR (Spotlight 400 - Perkin-Elmer) equipment in ATR mode was used in the region of 4000-500cm<sup>-1</sup>, with 32 scans and 4 cm<sup>-1</sup> resolution.

### Energy Dispersive X-Ray Spectroscopy (EDS)

Energy Dispersive X-Ray Spectroscopy is a chemical analysis technique. The EDS technique detects x-rays emitted from the specimen during bombardment by an electron beam to characterize the elemental composition of the analyzed volume.

## RESULTS

### Scanning Electron Microscopy (SEM)

Scanning electron microscopy (SEM) images were obtained from the experimental groups described in the methodology, which can be observed in Figures 2 and 3.

The applied electrospinning technique resulted in the synthesis of misaligned NFs for all groups.

### Measurement of the nanofiber diameter by software imageJ

After obtaining the SEM images (Figure 2 and Figure 3), ImageJ software was used to measure the NFs' diameter. Table 2 was used to analyze the distribution of diameters obtained for each experimental group.

In G1, the obtained NFs had diameters ranging from 97-254nm. However, the highest percentage of NFs had a diameter in the range of 128 to 160 nm, in which the mean value of the fibers was 174.46nm.

In G2, the obtained NFs had diameters ranging from 58-211nm. However, the highest percentage of NFs had a diameter in the range of 100 to 130nm, and the mean fiber value of this group was 123.57nm.

In G3, the obtained NFs had diameters varying between 117-239nm. However, the highest percentage of NFs had a diameter in the range of 150-190nm, and the mean value of the fibers in this group was 178.69nm.

In G4, the obtained NFs had diameters ranging from 82-327nm. However, the highest percentage of NFs had a diameter in the range of 82-123nm, and the mean value of the fibers in this group was 143.11nm.

In G5, the obtained NFs had diameters varying between 85-190nm. However, the highest percentage of NFs had a diameter in the range of 110-130nm, and the mean value of the fibers in this group was 129.73nm.

In G6, the obtained NFs had diameters varying between 83nm-392nm. However, the highest percentage of NFs had a diameter in the range of 125-170nm, and the mean value of the fibers in this group was 160.83nm.

**Table 2** - Mean and Standard Deviation of each group of nanofibers (all measurements are in nanometers)

	G1	G2	G3	G4	G5	G6
Mean (nm)	174.46	123.57	178.69	143.11	129.73	160.83
SD	25.96	27.07	24.749	40.69	22.07	54.06

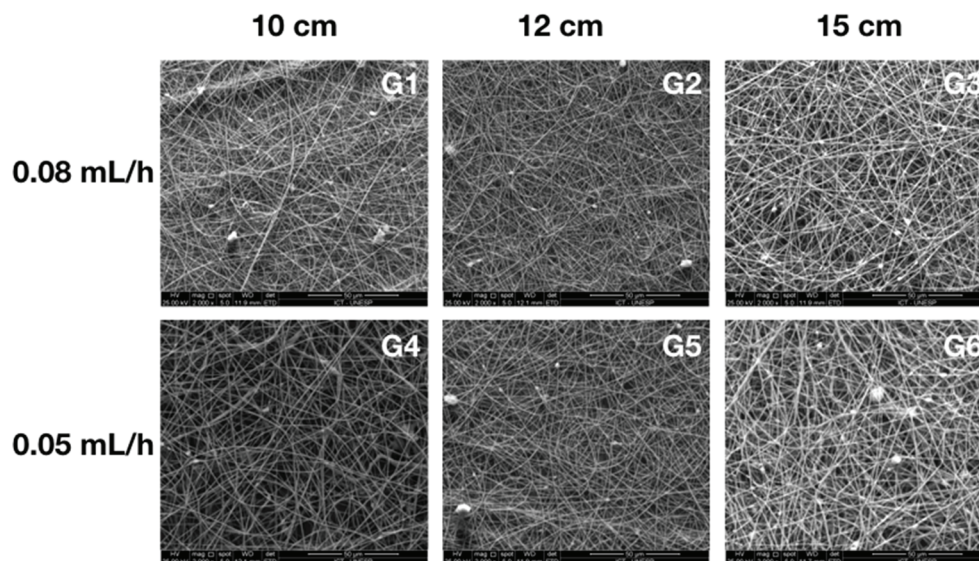


**Figure 2** - Photomicrography of the experimental conditions (2000x).

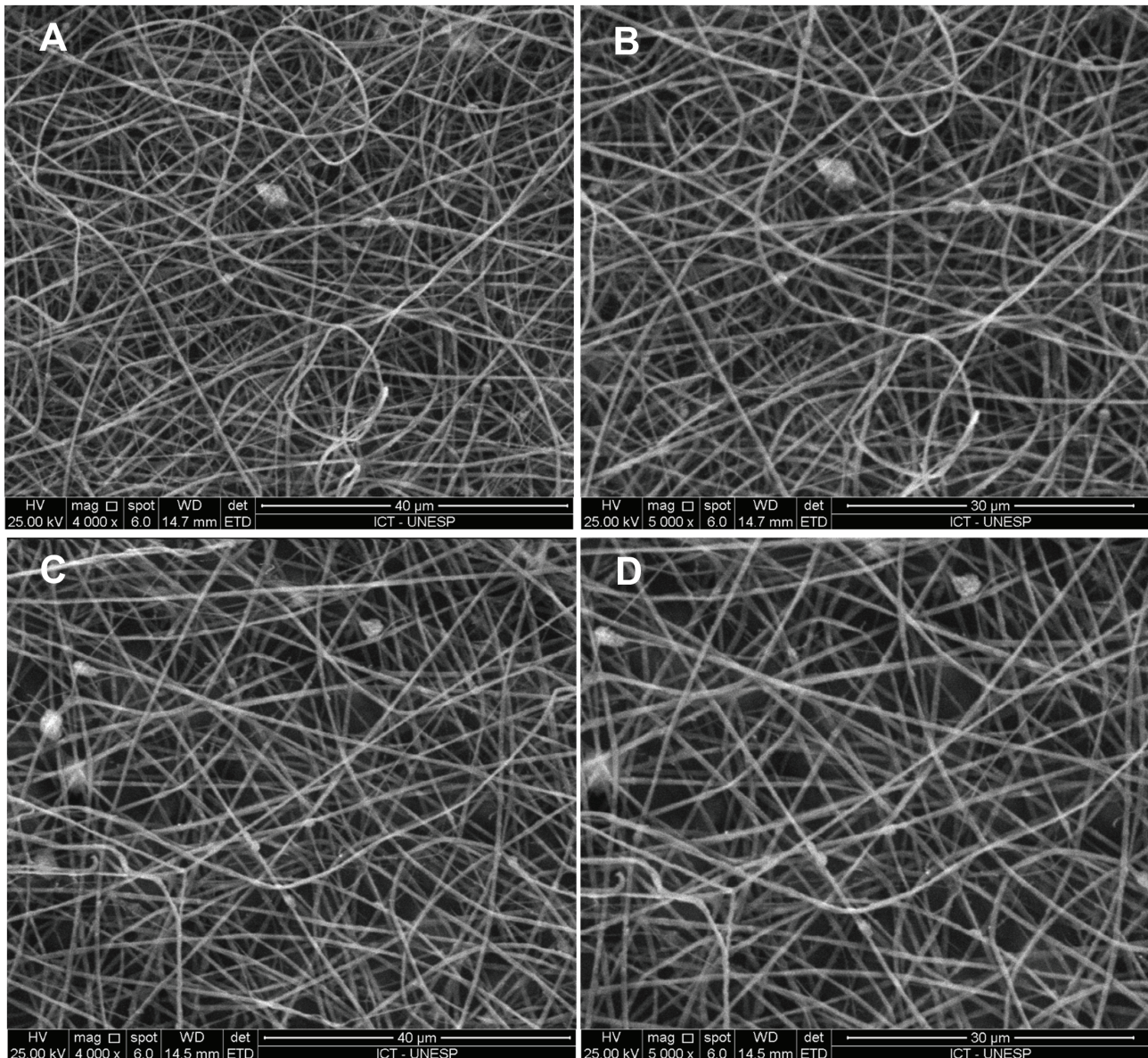


**Figure 3** - Photomicrography of the smaller diameters of the experimental conditions (4000x and 5000x).

### Fourier Transform Infrared Spectrophotometer

FTIR was performed to physically characterize the nanofibers obtained by the PEMA and TiO<sub>2</sub> blends. FTIR spectroscopy is important in investigating the structure of the compound, as it provides information on the interactions between the various constituent elements of polymer blends. Investigation is possible by this assay because the atoms

forming the molecules have specific vibration frequencies, which vary according to the structure, composition and mode of vibration of the specimen [18].

The following parameters were evaluated: distance of 12cm between needle tip and collector, flow rates of 0.05 and 0.08mLh<sup>-1</sup> and 17kV, corresponding to groups 2 and 5 evaluated by the SEM test and diameter measurement by ImageJ software, being considered the most

effective parameters in the synthesis of NFs. The of PEMA and PEMA/TiO<sub>2</sub> spectra in the flow rate condition of 0.05m mLh<sup>-1</sup> and the PEMA/TiO<sub>2</sub> in the flow rate condition of 0.08mLh<sup>-1</sup> overlap the graphs in the previous visual comparison of the obtained results.

According to the literature and chemical structure of PEMA, and very similar to poly (methyl methacrylate) (PMMA) [19], the difference between them is in the chain of the group allocated to methacrylate. PMMA contains the methoxy group (-OCH<sub>3</sub>) bonded to the carbonyl (C = O), while the PEMA has the ethoxy group (-OC<sub>2</sub>H<sub>5</sub>) bonded to the carbonyl.

The vibrational frequency of PEMA can be found in the literature. According to Venkatesh et al. (1985), the bands observed at 2991, 2942 and 2927cm<sup>-1</sup> have been attributed to C-H stretching overlapping the methylene (-CCH<sub>3</sub>) and ethylene (-OC<sub>2</sub>H<sub>5</sub>) groups. In the study by Sim LN et al. (2012), the characteristic peaks of PEMA due to the stretching of the carbonyl group [ $\nu$  (C = O)], deformation of CH<sub>2</sub> [ $\delta$  (CH<sub>2</sub>)], asymmetric O-C<sub>2</sub>H<sub>5</sub> flexion [ $\gamma$  (OC<sub>2</sub>H<sub>5</sub>)], torsion of [ $\tau$  (CH<sub>2</sub>)] and vibration asymmetry of COC stretching bond [ $\nu_a$  (COC)] are observed at 1723, 1476, 1446, 1388 and 1142cm<sup>-1</sup>, respectively.

Regarding titanium, the bands at 700, 643 and 550cm<sup>-1</sup> are characteristic of TiO<sub>2</sub> in the anatase crystalline form [20].

#### Energy Dispersive X-Ray Spectroscopy (EDS)

The specimen x-ray energy values from the EDS spectrum are compared with known characteristic x-ray energy values to determine the presence of an element in the specimen. Elements with atomic numbers ranging from that of beryllium to uranium can be detected.

EDS showed the presence of C and O in the nanofiber specimens, thus characterizing the presence of PEMA, while Ti was also found by recalibrating the presence of TiO<sub>2</sub> (Figure 5).

## DISCUSSION

Antimicrobial agents have been pursued as an alternative strategy for reducing initial microorganisms adhesion and biofilm formation on prosthesis surfaces [21,22]. Moreover, biomaterial characteristics such as composition and surface topography also influence the biofilm [22]. In this study, a synthesis pattern with the best biomimetic characteristics of PEMA scaffold with TiO<sub>2</sub> was studied.

The electrospinning technique produced nanofibers with a thinner diameter and consequently larger surface area than the conventional spinning processes [23]. Nanofibers can present beads which are considered a common problem, and whose occurrence depends on avoiding processing variables [24], as described by other studies [16]. The desired morphology would have uniform fibers without beads which would make its reproduction reliable, and a smaller diameter for obtaining hair surface area for higher storage and consequently delivery drugs [25].

The mean diameter of a nanofiber depends on the spinning parameters, but the solution concentration is the most crucial [26]. The solution concentration in this study was the same for the all specimens, and the mean diameters did not present a statistically significant difference between the groups, thus demonstrating that all parameter combinations were effective for the NF production.

In the electrospinning process, the jet goes against the collector as soon as the voltage exceeds the superficial energy of the solution. The jet may suffer instabilities in this stage, resulting in non-uniform nanofibers with a reticular aspect [27]. This formation can be observed in the C and F micrographs.

The 12 cm distance between the needle tip and the NF collector resulted in smaller diameters for the two evaluated flow ratios, and the 0.08 mLh<sup>-1</sup> flow rate resulted in NFs with the smallest diameter (123  $\mu$ m) (Figure 3). The adjustment in the parameters is essential

for NFs with desired morphology and diameter. The distance between the tip of the injector and the collector should be the minimum able to guarantee total solvent evaporation, and the maximum so that the electric field is effective in stabilizing the Taylor cone, and consequently in the formation of NFs [14,16].

By means of the diameters, we can suggest that the execution ratio did not change the graph pattern for the PEMA/TiO<sub>2</sub> blends. In addition, all components (PEMA and TiO<sub>2</sub>) can be found in the final version of the NF. This can be seen in Figures 4 and 5, in which we can detect the presence of characteristic TiO<sub>2</sub> and PEMA bands.

The electrospinning process produced

nanofibers with potential applications in many fields [28]. Nanofibers have been exploited as novel means for the controlled release of drugs because they have a surface area ratio by increased volume [13]. A drug delivery system is possible with scaffolds of biocompatible polymer matrices to deliver therapeutic agents [29]. The oral mucosa is an attractive site for administrating drug delivery because it is highly vascularized and has reduced enzymatic activity when compared to mucous, intestinal, rectal and nasal mucosa, and is less sensitive to damage and irritation when compared to nasal epithelium [30]. In this study, PEMA nanofibers with TiO<sub>2</sub> were produced aiming for the controlled release of the agent *in loco*, acting in the control and prevention of the *Candida albicans* microorganism.

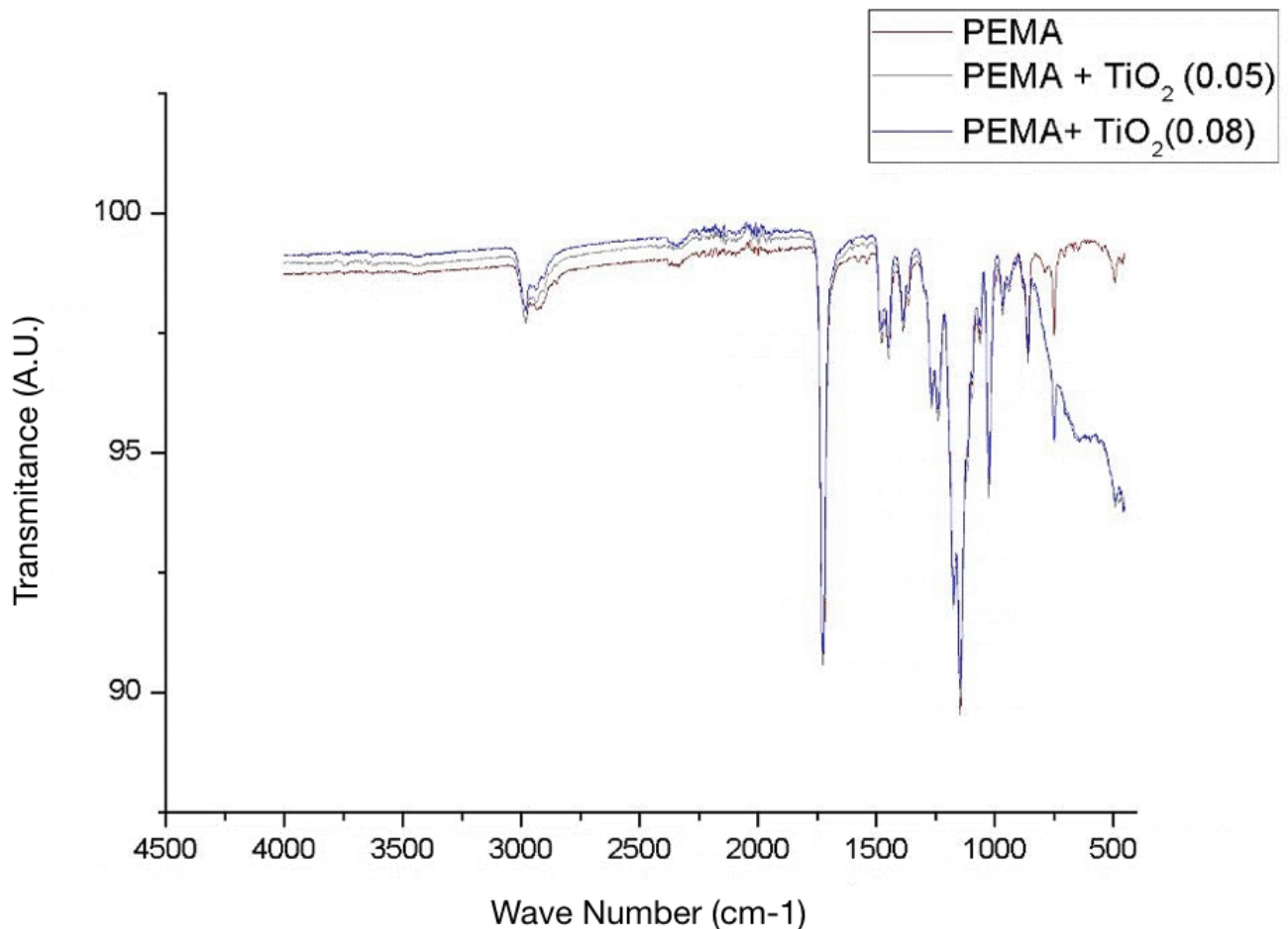
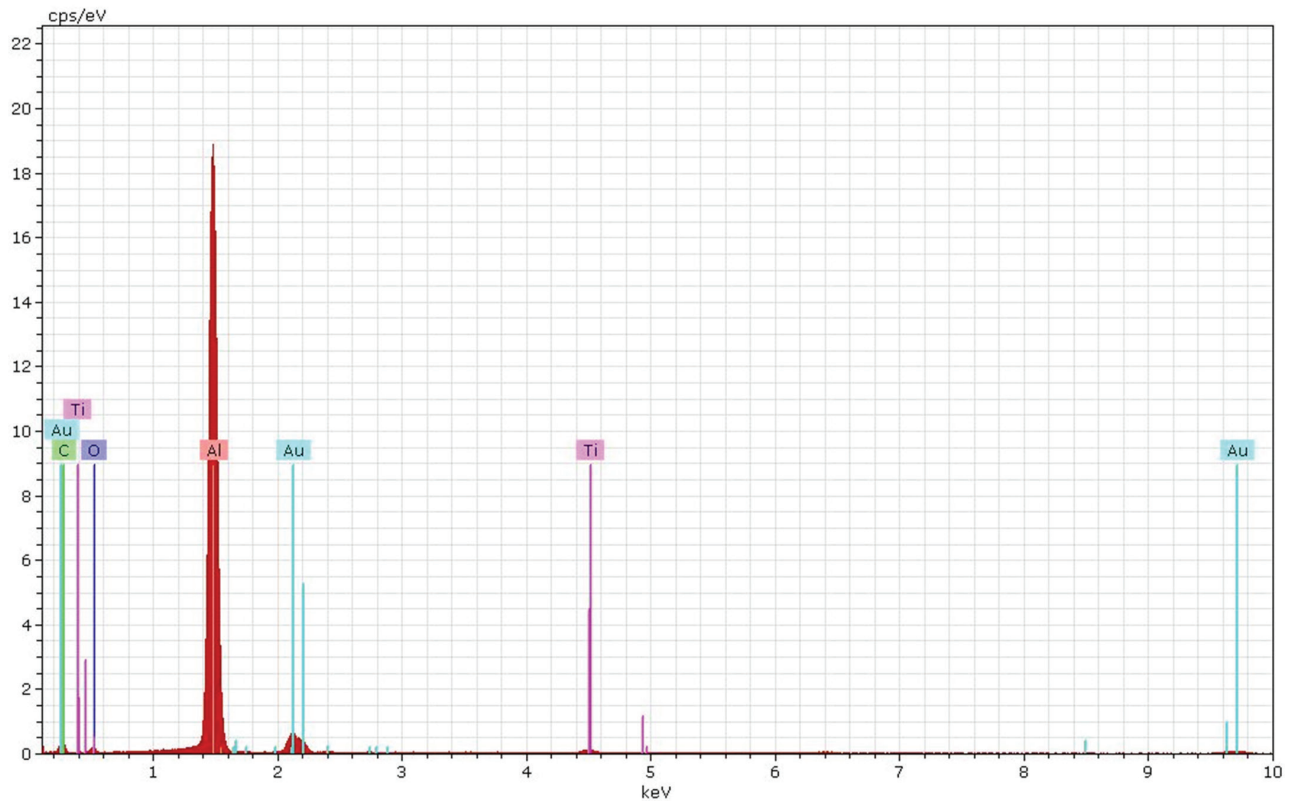


Figure 4 - FTIR Spectra



## Spectrum: Acquisition

El	AN	Series	unn. C [wt.%]	norm. C [wt.%]	Atom. C [at.%]	Error (1 Sigma) [wt.%]
Al	13	K-series	49.29	60.87	52.25	2.45
C	6	K-series	16.49	20.36	39.26	3.16
O	8	K-series	3.52	4.35	6.29	0.83
Au	79	M-series	10.57	13.05	1.53	0.46
Ti	22	K-series	1.11	1.37	0.66	0.07
Total:			80.97	100.00	100.00	

Figure 5 - EDS Spectra

The electrospinning technique was efficient for producing NFs containing PEMA and TiO<sub>2</sub>, while electrospinning parameters influenced the structural morphology. The most efficient parameters for producing NFs from the blends (PEMA and TiO<sub>2</sub>) was the distance of 12cm between the needle tip and

the NF collector for the two studied flow rates, maintaining the tension constant at 17kV; this standardization is very important for optimizing the in-scale production of these NFs. Regarding future perspectives, these NFs can be inserted in dental materials to obtain antifungal action.

## REFERENCES

- Chandra J, Kuhn DM, Mukherjee PK, Hoyer LL, McCormick T, Ghannoum MA. Biofilm formation by the fungal pathogen *Candida albicans*: development, architecture, and drug resistance. *J Bacteriol*. 2001 Sep;183(18):5385-94.
- Dorko E, Jenča A, Pilipčinec E, Danko J, Švický E, Tkáčiková L. *Candida*-associated denture stomatitis. *Folia Microbiol (Praha)*. 2001;46(5):443-6.
- Banting DW, Greenhorn P, McMinn J. Effectiveness of a topical antifungal regimen for the treatment of oral candidiasis in older, chronically ill, institutionalized, adults. *J Can Dent Assoc*. 1995 Mar;61(3):199-200, 203-5.
- Baena-Monroy T, Moreno-Maldonado V, Franco-Martinez F, Aldape-Barríos B, Quindos G, Sánchez-Vargas L. *Candida albicans*, *Staphylococcus aureus* and *Streptococcus mutans* colonization in patients wearing dental prosthesis. *Med Oral Patol Oral Cir Bucal*. 2005 Apr 1;10 Suppl 1:E27-39.
- Urban VM, De Souza RF, Galvao Arrais CA, Borsato KT, Vaz LG. Effect of the association of nystatin with a tissue conditioner on its ultimate tensile strength. *J Prosthodont*. 2006 Sep-Oct;15(5):295-9.
- Salim N, Moore C, Siliikas N, Satterthwaite J, Rautemaa R. Candidacidal effect of fluconazole and chlorhexidine released from acrylic polymer. *J Antimicrob Chemother*. 2013 Mar;68(3):587-92. doi: 10.1093/jac/dks452. Epub 2012 Nov 21.
- Kamikawa Y, Hirabayashi D, Nagayama T, Fujisaki J, Hamada T, Sakamoto R, et al. In vitro antifungal activity against oral *Candida* species using a denture base coated with silver nanoparticles. *J Nanomater*. 2014(9177):1-6.
- Nam KY. Characterization and bacterial anti-adherent effect on modified PMMA denture acrylic resin containing platinum nanoparticles. *J Adv Prosthodont*. 2014 Jun;6(3):207-14. doi: 10.4047/jap.2014.6.3.207. Epub 2014 Jun 24.
- Su W, Wei S, Hu S, Tang J. Preparation of TiO<sub>2</sub>/Ag colloids with ultraviolet resistance and antibacterial property using short chain polyethylene glycol. *J Hazard Mater*. 2009 Dec 30;172(2-3):716-20. doi: 10.1016/j.jhazmat.2009.07.056. Epub 2009 Jul 22.
- Wan Y, Zhang D, Wang Y, Qi P, Wu J, Hou B. Vancomycin-functionalised Ag@ TiO<sub>2</sub> phototoxicity for bacteria. *J Hazard Mater*. 2011 Feb 15;186(1):306-12. doi: 10.1016/j.jhazmat.2010.10.110. Epub 2010 Nov 10.
- Mu R, Xu Z, Li L, Shao Y, Wan H, Zheng S. On the photocatalytic properties of elongated TiO<sub>2</sub> nanoparticles for phenol degradation and Cr (VI) reduction. *J Hazard Mater*. 2010 Apr 15;176(1-3):495-502. doi: 10.1016/j.jhazmat.2009.11.057. Epub 2009 Nov 13.
- Casemiro LA, Martins CHG, Pires-de-Souza FdC, Panzeri H. Antimicrobial and mechanical properties of acrylic resins with incorporated silver-zinc zeolite – part I. *Gerodontology*. 2008 Sep;25(3):187-94. doi: 10.1111/j.1741-2358.2007.00198.x. Epub 2008 Jan 13.
- Huang Z-M, Zhang Y-Z, Kotaki M, Ramakrishna S. A review on polymer nanofibers by electrospinning and their applications in nanocomposites. *Comp Sci Technol*. 2003;63(15):2223-53.
- Li D, Xia Y. Electrospinning of nanofibers: reinventing the wheel? *Adv Mater*. 2004;16(14):1151-70.
- Doshi J, Reneker DH. Electrospinning process and applications of electrospun fibers. *J Electrostat*. 1995;35(2-3):151-60.
- de Souza JR, Sato TP, Borges ALS. Scaffold architecture for dental biomaterials: influence of process parameters on the structural morphology of chitosan electrospun fibers. *Braz Dent Sci*. 2017;20(4):100-5.
- Dzenis Y. Spinning continuous fibers for nanotechnology. *Science*. 2004;304(5679):1917-9.
- Chia L, Ricketts S. *Basic Techniques and Experiments in Infrared and Ft-ir Spectroscopy*: Perkin Elmer; 1988.
- Ramesh S, Wen LC. Investigation on the effects of addition of SiO<sub>2</sub> nanoparticles on ionic conductivity, FTIR, and thermal properties of nanocomposite PMMA-LiCF<sub>3</sub>SO<sub>3</sub>-SiO<sub>2</sub>. *Ionics*. 2010;16(3):255-62.
- Chen J, Zhou Y, Nan Q, Sun Y, Ye X, Wang Z. Synthesis, characterization and infrared emissivity study of polyurethane/TiO<sub>2</sub> nanocomposites. *Appl Surf Sci*. 2007;253(23):9154-8.
- Monteiro DR, Gorup LF, Takamiya AS, Ruvollo-Filho AC, de Camargo ER, Barbosa DB. The growing importance of materials that prevent microbial adhesion: antimicrobial effect of medical devices containing silver. *Int J Antimicrob Agents*. 2009 Aug;34(2):103-10. doi: 10.1016/j.ijantimicag.2009.01.017. Epub 2009 Mar 31.
- Teughels W, Van Assche N, Sliepen I, Quirynen M. Effect of material characteristics and/or surface topography on biofilm development. *Clin Oral Implants Res*. 2006 Oct;17 Suppl 2:68-81.
- Chew S, Wen Y, Dzenis Y, Leong KW. The role of electrospinning in the emerging field of nanomedicine. *Curr Pharm Des*. 2006;12(36):4751-70.
- Bhardwaj N, Kundu SC. Electrospinning: a fascinating fiber fabrication technique. *Biotechnol Adv*. 2010 May-Jun;28(3):325-47. doi: 10.1016/j.biotechadv.2010.01.004. Epub 2010 Jan 25.
- Sundar SS, Sangeetha D. Fabrication and evaluation of electrospun collagen/poly (N-isopropyl acrylamide)/chitosan mat as blood-contacting biomaterials for drug delivery. *J Mater Sci Mater Med*. 2012 Jun;23(6):1421-30. doi: 10.1007/s10856-012-4610-x. Epub 2012 Apr 3.
- Deitzel JM, Kleinmeyer J, Harris D, Tan NB. The effect of processing variables on the morphology of electrospun nanofibers and textiles. *Polymer*. 2001;42(1):261-72. doi: 10.1016/S0032-3861(00)00250-0.
- Koombhongse S, Liu W, Reneker DH. Flat polymer ribbons and other shapes by electrospinning. *J Polym Sci Part B: Polym Phys*. 2001;39(21):2598-606. doi: 10.1002/polb.10015.
- Matthews JA, Wnek GE, Simpson DG, Bowlin GL. Electrospinning of collagen nanofibers. *Biomacromolecules*. 2002;3(2):232-8.
- Kost J, Langer R. Responsive polymeric delivery systems. *Adv Drug Deliver Rev*. 2012;64:327-41.
- Rossi S, Sandri G, Caramella CM. Buccal drug delivery: a challenge already won? *Drug Discov Today Technol*. 2005 Spring;2(1):59-65. doi: 10.1016/j.ddtec.2005.05.018.

**Jéssica Dias Santos**  
(Corresponding address)

PhD student in Prosthodontics, Institute of Science and Technology of Sao Jose dos Campos, São Paulo State University (UNESP), Sao Jose dos Campos, Brazil.  
E-mail address: jediassantos@gmail.com

Date submitted: 2018 Jul 23

Accept submission: 2019 Jan 21